NJC

Organosilane sulfonated Graphene oxide in the Biginelli and Biginelli-like reactions

SCHOLARONE™
Manuscripts

Journal Name

ARTICLE TYPE

Organosilane sulfonated Graphene oxide in the Biginelli and Biginelli-like reactions

Javad Safari*, Soheila Gandomi-Ravandi, Samira Ashiri

Organosilane sulfonated graphene oxides (SSi–GO) have been synthesized by a two-step procedure involving the grafting of graphene oxide (GO) with 3-chloropropyltriethoxysilane (CCPTES) and subsequent oxidation using sulfanilic acid. It is shown that organosilane sulfonated graphene oxide (SSi–GO) exhibits a superior catalytic performance to produce dihydropyrimidines (DHPMs) in the Biginelli

10 and Biginelli-like reactions. This stronger acidity corresponds to the cooperative effects of the aryl sulfonic acid groups and other kinds of acid sites (carboxylic acids). However, the acidic functionalities bonded to the SSi–GO surface are stable under the catalytic reaction conditions resulting its efficient reuse.

Introduction

15 Graphite oxide (GtO) is a carbonaceous layered material consisting of hydrophilic oxygenated graphene sheets (graphene oxide sheets). Generally, bulk graphite oxide can be prepared by the oxidative treatment of purified natural graphite powders using the modified Hummers method. This involved the use of strong

20 concentrated oxidizing acids (HNO_3 and H_2SO_4) and strong oxidizing salts (potassium permanganate). [1] Despite the retention of the layered structure, Graphite oxide has much lighter color than graphite powder owing to the loss of electronic conjugation afforded by the oxidation. Graphite oxides contain covalently

25 attached oxygen-containing groups such as sp^3-hybridized carbons containing hydroxyl and epoxide functional groups on above and below each sheet (the basal planes) as major components, and sp^2-hybridized carbons containing carbonyl and carboxyl groups located at the edges of the basal planes and hole

30 defects as minor components. [2–5] These oxygen functionalities make GtO sheets strongly hydrophilic, therefore mild sonication of graphite oxide (GtO) in both aprotic polar solvents and water results monolayer exfoliation to form homogeneous and stable aqueous dispersions containing sheets with atomic thickness. [6]

35 Indeed, GtO consists graphene oxide sheets with both covalently bound oxygen and non-covalently bound water between the carbon layers. Therefore, Graphene oxide -the oxygenated form of a monolayer graphene platelet- should be noticed as an amphiphile with a largely hydrophobic basal plane (polyaromatic

40 islands of unoxidized benzene rings) and hydrophilic edges (–COOH groups). [7-10] GO sheets are composed of planar and graphene-like aromatic domains with a hexagonal ring based carbon network in chair configuration bearing oxygen functional groups. [11] GO is a single-layer of graphite oxide with two-

45 dimensional network of sp^2- and sp^3-hybridized carbon atoms, while an ideal graphene sheet consists 100% sp^2-bonded carbon

atoms. [12] The unique electronic structure of Graphene oxide (GO) is heterogeneous owing to presence of mixed sp^2 and sp^3 hybridizations. [13] The availability of oxygen-containing

50 functional groups on the GO sheets allows it to be functionalized with a wide range of organic and inorganic materials in covalent or non-covalent and/or ionic approaches. [14] Thus, GO is a significant building block to prepare various functional materials. [15] These oxygen functional groups afford mild acidic and

55 oxidative properties for GO, [16] and further functionalization can make stronger acid sites on these carbons. [17-19] Unique properties of Graphene oxide (GO) including 2D structure, high stability and high surface areas make it an novel type of promising carbocatalysts which their catalytic performance can be promoted

60 with functionalities to both sides of the carbon sheets. [20] The functionalized GO has great potential for use in biosensing, [21] drug delivery, [22-24] bio-analysis, [25] gene delivery and bioimaging, [26] photothermal therapy, [27] hydrogen storage, [28] transparent film, [29] high efficiency catalysis, [30-32] electronics and optoelectronics,

65 [33] and chemical and biochemical sensors. [34] It is because of its exclusive characteristics such as high mechanical strength, [35] good water dispersibility, [36] facile surface modification, [37] and photoluminescence. [38]

Heterocyclic moiety is a key structure in many bioactive natural

70 and therapeutic products. Nitrogen heterocycles are important branches of pharmacologically active substances and they have been utilized as significant precursors in the synthesis of novel drugs. Out of the five major bases in nucleic acids, three i.e Cytosine, Uracil and Thymine are pyrimidine derivatives which

75 are found in DNA and RNA. [39,40] Therefore, pyrimidines have become very important in the world of synthetic organic chemistry. [41] 3,4-Dihydropyrimidinones as biologically active compounds have been extensively used as drug-like scaffolds due to their pharmacological and therapeutic properties. [42] Their

80 derivatives such as monastrol, enastron, piperastrol, [43] amlodipine

and nicardipine [44] have been developed as drugs. Biginelli reaction is one of the most efficient and straightforward procedures to obtain the DHPMs including the acid-catalyzed three component condensation in one-pot. The efficiency of this process is greatly limited owing to strong acidic and harsh reaction conditions. [45] Thus, new modified routes have been developed to improve the efficiency of the Biginelli reaction in the presence of highly active, stable, and friendly environments catalysts.

Herein, we report the highly efficient activity of organosilane sulfonated graphene oxide (SSi–GO) as an effective catalyst to prepare pyrimidinones (Schemes 1 and 2). First, the sulfonated graphene oxide nanosheets are prepared through facile covalent functionalization with sulfanilic acid. The functionalized GO is then used as highly active, selective, reusable and stable catalyst to produce pyrimidinones. The carboxylic acid and sulfonic acid groups are present in SSi–GO are potentially active sites for its superior catalytic performance. However, the organosilane sulfonated graphene oxide has not yet been used as heterogeneous catalysts in the Biginelli reaction.
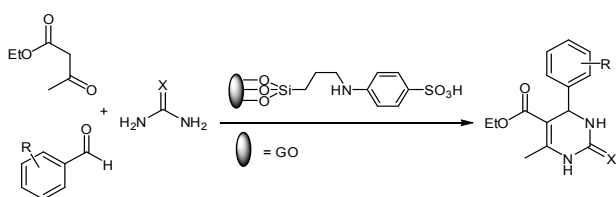
Scheme 1. SSi–GO-catalyzed synthesis of dihydropyrimidinones
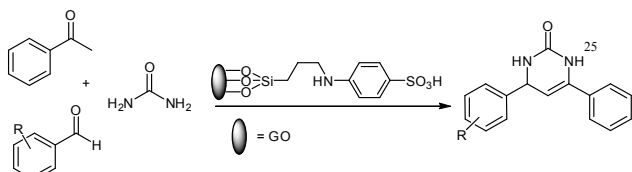
**Scheme 2.** SSi–GO-catalyzed synthesis of diarylpyrimidinones

Experimental

Materials and methods

Chemical reagents were purchased from Merck and Aldrich with high purity and used as received without further purification. The completion of reactions were checked by TLC technique on silica gel plates in the solvent system petroleum ether–EtOAc (V/V = 7:3). Melting points (ºC) were determined in open-glass capillary on an Electrothermal MK3 apparatus and are uncorrected. A Perkin Elmer FT–IR 550 spectrophotometer was used for recording IR spectra using potassium bromide pellets in the range 400-4000 cm^{-1}. Proton and carbon NMR spectra were recorded on a Bruker DRX–400 spectrometer operated at 400 MHz using CDCl$_3$ as solvent and TMS as interior standard. X-ray diffraction patterns were performed on a Holland Philips Xpert X-ray diffractometer with CuK, (radiation, λ= 0.154056 nm) radiation, at a scanning speed of 2º/min from 10º to 100º (2θ). Scanning electron microscopy (SEM) was performed on a Quanta 200 SEM operated at a 20 kV accelerating voltage. The samples were prepared for SEM by spreading a small drop containing GO onto

a silicon wafer and by drying it almost completely in air at room temperature for 2 h; it was then transferred onto SEM conductive tape. The transferred sample was coated with a thin layer of gold before measurement. Sonication was performed in Shanghai Branson-BUG40-06 ultrasonic cleaner (with a frequency of 35 kHz and a nominal power of 200 W). A circulating water bath (DC2006, Shanghai Hengping Apparatus Factory) was adopted with an accuracy of 0.1 K to keep constant the reaction temperature.

General procedure for the preparation of Graphene Oxide (GO):
The graphene oxide (GO) nanosheets were prepared from natural graphite power using the modified Hummer's method. [1] In a typical synthesis process, graphite powder (3 g) and sodium nitrate (NaNO$_3$, 1 g) were slowly added to a solution of H$_2$SO$_4$ 98 % (46 mL) while stirring in an ice bath at 0–5 ºC (15 min). Under vigorous stirring, potassium permanganate (KMnO$_4$, 6 g) were slowly added to the suspension at 10–15 ºC for 2 h. The resulting mixture stirred continuously at 35 ºC for another 30 min. Subsequently, distilled water (138 mL) was slowly added to the reaction vessel under vigorous stirring, which led to a color change to yellow. Then, the reaction mixture was treated with 30 % hydrogen peroxide (H$_2$O$_2$, 18 mL). The resultant brown solution was washed with 10% hydrochloric acid (HCl) solution, after that centrifuged for several times. The brown graphite oxide was collected by filtration and dried under the vacuum at 60 ºC for 24 h. To prepare graphene oxide (GO), 100 mg graphite oxide was dispersed in distilled water (100 mL) and sonicated in ultrasonic bath cleaner (100 W) for hours to exfoliate graphitic oxide until the solution became clear. Indeed, the graphene oxide (GO) in aqueous solution was generated by the oxidization and subsequently exfoliation of graphite. Afterwards, the GO solution was centrifuged for 10 min to remove any unexfoliated graphitic oxide. The dry GO was obtained after drying in vacuum oven at 80 ºC for 24 h. Scheme 3 briefly illustrates the used procedure to synthesize GO.
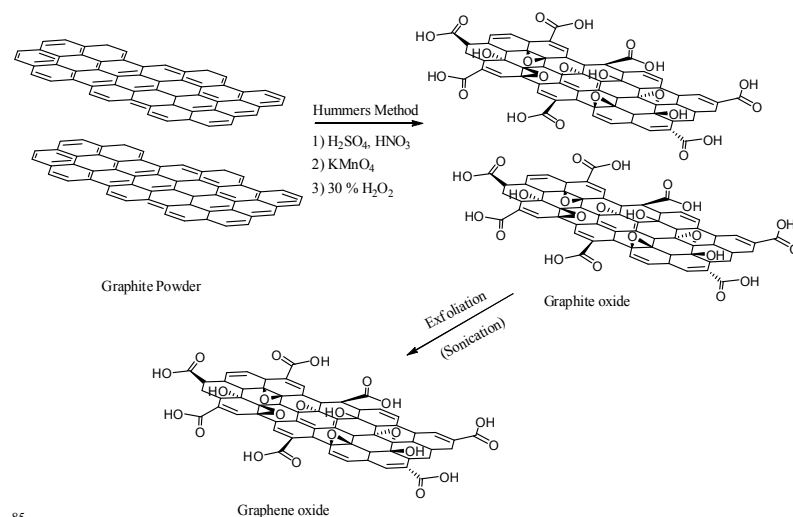

Scheme 3. Schematic model of the used procedure to synthesize graphene oxide

General procedure for the preparation of organosilane

Sulfonated graphene oxide (SSi–GO):

The process for synthesizing organosilane sulfonated graphene oxide from graphene oxide was carried in the following. The functionalized, chemically converted graphene nanosheets (SSi–GO) can be synthesized via the covalent interaction between GO and sulfanilic acid. In a typical procedure, the functionalization of GO (F-GO) nanosheets was performed using 3-chloropropyltriethoxysilane (CPTES) as the sulfonic acid functional group precursor. The reaction was carried out in toluene at temperature of 110 ºC under reflux conditions for 24 h, with ratios of 3:1:2 of toluene, GO and CPTES, respectively. Afterwards, the chloro groups grafted onto the GO nanosheets to achieve chlorofunctionalized GO (ClSi–GO). The prepared samples were filtered and washed three times with ethanol to remove the precursor residue. Samples were then dried at temperature of 80 ºC for 8 h. Finally, sulfanilic acid (1.5 g) was added to a mixture of ClSi–GO (1 g) and triethylamine (1.2 mL, 8.6 mmol) in 30 mL of toluene. The solution was continuously stirred at 110 ºC under reflux condition for 48 h to produce the SSi–GO. After the reaction, the mixture was washed with toluene and chloroform for several times and then collected by centrifuge and dried in a vacuum oven at 80 ºC for 24 h. The synthesis of organosilane sulfonated graphene oxide was described in several steps in Scheme 4.
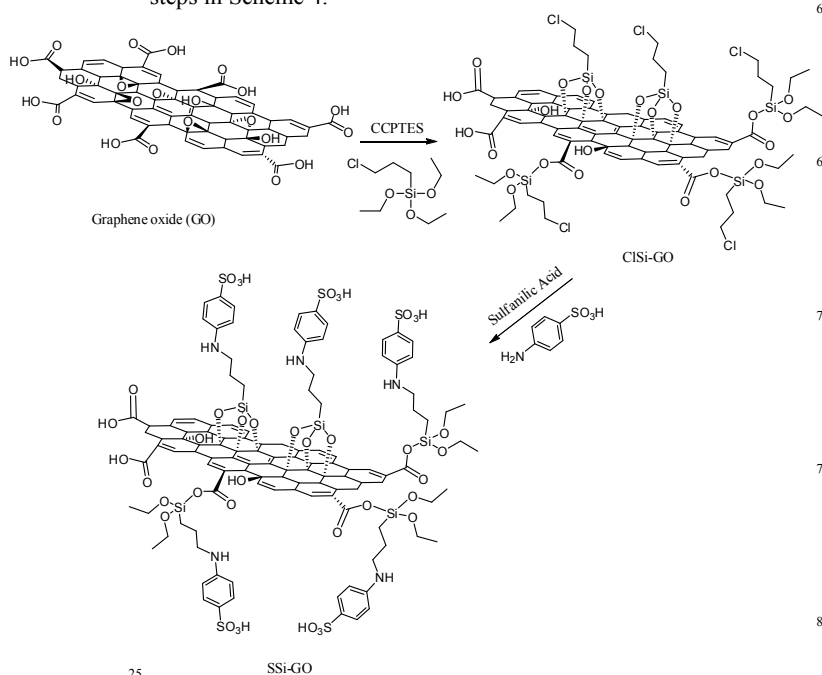
Scheme 4. Schematic illustration to prepare organosilane sulfonated graphene oxide

General procedure for the preparation of pyrimidinone derivatives

Solution of aromatic aldehyde (1 mmol), ethyl acetoacetate (aromatic ketone) (1 mmol) and urea or thiourea (1.5 mmol) in 5 ml of ethanol was stirred and refluxed at 80 ºC in the presence of the SSi–GO (0.1 g). The completion of the reaction was determined on TLC plates using ethyl acetate / petroleum ether mixture as a mobile phase. After completion, the mixture was cooled to room temperature, then crushed ice was added to

precipitate the product. The yellow solid precipitate was separated by filtration through a Buckner funnel and washed with cold water to remove excess of urea and dried under vacuum. In addition, it was further purified by recrystallization from hot ethanol to afford pure pyrimidinones. Then, the filtrate obtained was concentrated under reduced pressure to recover catalyst which could be reused in subsequent experiments. The recovered catalyst was washed with water, dried under vacuum oven at 90 ºC for about 3 h and reused for subsequent reaction.

Results and discussion

The preparation of graphene oxide nanosheets from graphite powder via Hummers method affords hydrophilic oxygen-containing functional groups such as carboxyl, epoxy, and hydroxyl on the surfaces of GO nanosheets, which can stabilize dispersion of these sheets in aqueous media. [48] Graphene oxide, which is introduced as the oxidized graphene, was modified by treatment with sulfanilic acid to afford sulfur-containing acid groups onto the carbon surface.

Screening of reaction conditions

The catalytic activity of organosilane sulfonated graphene oxide was investigated to produce dihydropyrimidinones. Initially, to evaluate the effect of catalyst, the reaction of benzaldehyde, ethyl acetoacetate, and urea in the presence and absence of an organosilane sulfonated graphene oxide nanocatalyst under reflux conditions was selected as a model reaction. The results are summarized in Table 1. It could be seen that without any catalysts was obtained no desirable DHPMs product even after prolonging reaction time (Table 1, entry 1). It indicated that the catalyst is necessary for this reaction. The yield increased linearly with increase in the amount of catalyst. Hence, 0.1 g of the catalyst was used in the reaction. It should be noted that the high catalytic activity of solid acid of SSi–GO was attributed to the quantity and type of acidic groups and high surface area. In other experiments, the same reaction carried out with the different amounts of urea in the presence of the same quantity catalyst (Table 2). Based on these results, the yield increased with the addition of urea and the optimal amounts of urea was 1.5 mmol. Thus, the best result was obtained with 1.0:1.0:1.5 molar ratios of aldehyde, 1,3-dicarbonyl compounds, urea or thiourea, and 0.1 g of SSi–GO.

Table 1. The effect of various amounts of catalyst for Biginelli reaction

Entry	Catalyst (g)	Time (min)	Yield (%)
1	–	50	–
2	0.05	40	83
3	0.1	20	94
4	0.2	25	92
5	0.3	20	94

The yield was calculated according to limiting factor (aldehyde)

Table 2. Optimization of amount of urea for the synthesis of DHPMs

Entry	Urea (mmol)	Yield (%)
1	1	60
2	1.5	94
3	2	92
4	2.5	90

The yield was calculated according to limiting factor (aldehyde)

The potency of the reaction was influenced by temperature. It was indicated that the reaction did not proceed at room temperature (Table 3, entry 1). Furthermore, it was observed that the yield of the reaction increased with the increasing of the reaction temperature ranging from 60 to 80 ºC (entries 2–4), but there was not much change when above 80 ºC.

Table 3. Optimization of reaction temperature in the synthesis of DHPMs

Entry	Temperature (ºC)	Yield (%)
1	r.t.	–
2	60	65
3	70	79
4	80	94
5	100	89

The yield was calculated according to limiting factor (aldehyde)

Next, the effect of various solvents on the improvement of reaction was tested. Typically, solvents such as H_2O, CH_3CN, DMF, EtOH and CH_2Cl_2 were selected for comparison. As shown, the polar solvents such as acetonitrile, H_2O and EtOH resulted good yields, while low yield of the product was obtained using DMF and CH_2Cl_2 (Table 4, entries 5,6). This may be attributed to the better solubility of the starting materials in the polar solvents. In comparison with aprotic solvents, a significant increase in the yield of the product was obvioused in shorter time period when the model reaction was occurred under solvent-free conditions. The highest yield of the product was obtained in EtOH as a protic and polar solvent within 20 min, but the reaction in other solvents afforded low yields in longer reaction times.

Table 4. Effect of various solvents on the Biginelli reaction

Entry	Solvent	Time (min)	Yield (%)
1	Solvent-free	35	80
2	Water	40	84
3	EtOH	20	94
4	CH_3CN	30	89
5	DMF	35	65
6	CH_2Cl_2	40	60

The yield was calculated according to limiting factor (aldehyde)

The most important feature of the present reaction is the recyclability of the catalyst. Subsequently, the recycling and reusability performance of SSi–GO nanocatalyst were investigated with the model reaction under the optimal conditions. After the catalytic reaction, water was added and the recovered catalyst was removed from the reaction mixture by filtration and washed with ethanol, and dried under vacuum at 90 ºC for 3 h. The recovered catalyst was reused five times without significant loss of catalytic activity. These results show that the catalyst is very stable. This observation strongly confirms the high recycling efficiency of the nanocatalyst which is a significant property in economical and environmental points of view.

Figure 1. Reusability of catalyst for the synthesis of **4a**

The results were tabulated to compare the efficiency of the present catalyst with some of the reported catalysts for the promotion of the synthesis of DHPMs. The present method was more efficient according to Table 5.

Table 5. Comparative study with published methods

Entry	Catalyst	Condition	Time (min)	Yield (%)	Ref.
1	PTA@MIL-101	Solvent free, 100 ºC	60	90	49
2	Cu@PMO-IL	Solvent free, 70 ºC	50	96	50
3	[TEBSA]HSO₄	Solvent free, Reflux	75	88	51
4	PPA	Solvent free, grinding	25	84	52
5	Nano-γ-Fe₂O₃-SO₃H	Solvent-free, 60 ºC	180	91	53
6	SiO₂-BaCl₂/ SF	Solvent-free, 85 ºC	45	93	54
7	Mn@PMO-IL	Solvent-free, 70 ºC	45	97	55
8	SiO₂-H₂PO₃	Solvent-free, 60 ºC	150	92	56
9	ErCl₃	Solvent-free, 120 ºC	30	92	57
10	SSi–GO	Reflux, 80 ºC	20	94	This Study

To investigate the substrates scope, the reactions were carried out with various aldehydes, 1,3-dicarbonyl compounds (acetophenones), and urea (or thiourea) catalyzed by SSi–GO in the optimal conditions. The results are shown in Tables 6 and 7. The reactions proceeded very efficiently within relatively short reaction time. The results illustrate that the type and position of the substituent have no significant effect on the activity of the catalyst and the reaction yield. These observations confirm high efficiency of the nanocatalyst to convert an extensive range of aldehyde substrates to a series of structurally diverse pyrimidinones in high purity. Additionally, thiourea was applied instead of urea to successfully provide the corresponding 3,4-dihydropyrimidin-2(1*H*)-thiones in good yields (Table 6, entries 10, 11). It is essential to note that the methodology was also successfully used for acetophenone substrates and corresponding adducts obtained in good yields. However, ketones required a longer reaction time (Table 7). The products were confirmed by comparing their melting point with authentic samples, FTIR and ^{1}H NMR spectroscopies.

Table 6. Synthesis of 3,4-dihydropyrimidin-2(1*H*)-one / thiones in the presence of SSi–GO catalyst under reflux conditions

Entry	Aldehyde	X	Product	Mp (ºC) Obs.	Mp (ºC) Lit.	Time (min)	Yield (%)
1	H	O	**4a**	200–202	200–201 [58]	20	94
2	4-Cl	O	**4b**	211–215	209-211 [59]	20	96
3	4-Me	O	**4c**	213–216	212-214 [60]	25	90
4	2-OH	O	**4d**	201–203	200–202 [61]	25	89
5	2-Cl	O	**4e**	215–218	216-218 [61]	27	91

6	2-F	O	4f	239–240	233-235 [62]	30	98
7	Thiophene	O	4g	215–217	215-217 [63]	20	92
8	3-NO$_2$	O	4h	229–230	229-231 [64]	23	94
9	4-NMe$_2$	O	4i	230-232	230-232 [65]	35	95
10	Thiophene	S	4j	216–217	215–216 [64]	30	90
11	H	S	4k	197–199	199–200 [66]	25	93

The yield was calculated according to limiting factor (aldehyde)

Table 7. Synthesis of diarylpyrimidin-2(1H)-ones in the presence of SSi–GO catalyst under reflux conditions

Entry	Aldehyde	Ketone	X	Product	Mp (ºC)		Yield (%)
					Obs.	Lit.	
1	H	H	O	6a	229–231	228–230 [67]	89
2	3,4-(OMe)$_2$	H	O	6b	245–246	243–245 [67]	90
3	3-OMe	H	O	6c	258–259	257–258 [67]	93
4	4-Cl	H	O	6e	268–269	267–269 [68]	98
5	4-Me	H	O	6f	249–251	248–250 [67]	87
6	4-OMe	H	O	6g	260–261	259–261 [67]	92
7	2-OMe	H	O	6h	265–267	266–267 [67]	89
8	4-OH	H	O	6i	256–258	257–258 [68]	77
9	2,4-Cl$_2$	H	O	6j	270–272	271–274 [67]	83
10	2-Cl	H	O	6k	263–264	264–265 [67]	91

5 The yield was calculated according to limiting factor (aldehyde)

Structural characterization of catalyst

The crystalline phases of graphite and graphite oxide samples prepared were investigated by the X-ray diffraction (XRD) 10 patterns shown in Figure 2. It can be seen in Fig. 2 that the natural graphite presented the very strong diffraction peak at $2\theta = 26.0º$ with (002) plane of graphite. The diffraction peak at around $2\theta = 43.1º$ is related to the (100) plane of the hexagonal structure of carbon. [69] Spectrum of graphite oxide after oxidation for 30 15 min exhibited the same peak but a little bit weaker than raw graphite and another peak at $2\theta = 11.7º$ appeared. However, after oxidation for 45 min, the peak becomes even weaker. It can be observed that after complete oxidation, the sharp diffraction peak disappeared in graphite nanosheets ($2\theta = 26.0º$), and a new 20 diffraction peak ($2\theta = 11.7º$ with 0.8 nm d-spacing corresponds to the (001) reflection) appeared in Graphite oxide, indicating the damage of the regular crystalline pattern of the graphite during the oxidation. The characteristic diffraction peak (001) of graphite oxid nanosheets and its increased d-spacing is associated 25 to introduce oxygenated functional groups attached on both sides and edges of carbon sheets as well as water molecules trapped in the interlayer galleries of hydrophilic Graphite oxide.
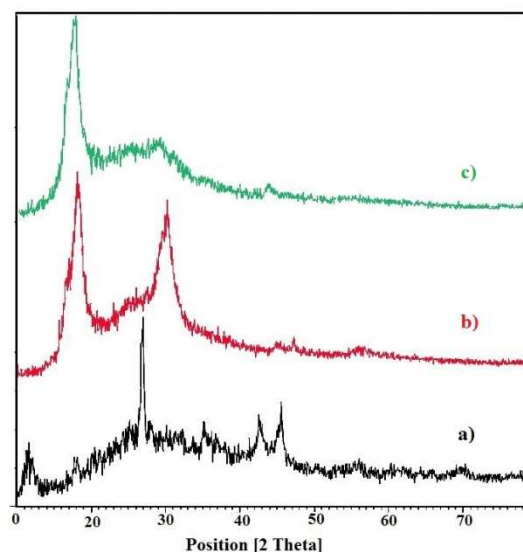

30 **Figure 2.** X-ray diffraction patterns of (a) graphite, (b) Graphite oxide after oxidation for 30 min and (c) Graphite oxide after oxidation for 45 min

Figure 3 shows typical Scanning electron microscopy (SEM) 35 images of the GtO and GO. Indeed, SEM images show the structures and morphology of graphite oxide before (Figs. 3a,b) and after (Figs. 3c,d) exfoliation. Compared with the graphite oxide which is a laminar compound with layers stucking together, graphene oxide exhibits relatively rougher surface and crumpling 40 features with clear layers. The atomic scale roughness rises from structural defects (sp^3 bonding) generated on the originally atomically flat graphite oxide sheet. It can be identified that GO nanosheets are relatively exfoliated and wrinkled and afforded an increase in the distance between adjacent sheets and reduction in 45 interaction between sheets. This increased spacing is considerably different depending on the amount of water intercalated within the stacked-sheet structure. [70] These factors have potential advantages as the active sites, which can be easily produced on both sides of the two dimensional graphene oxide sheets.
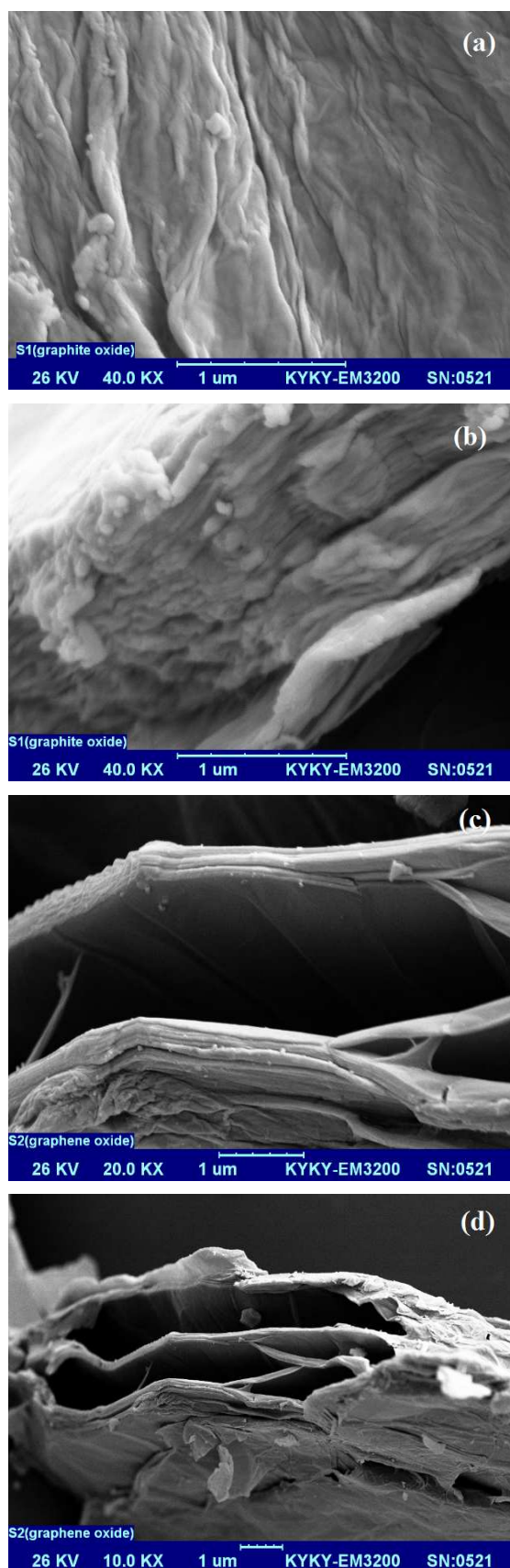
50

Figure 3. SEM images (a) and (b) Graphite oxide, (c) and (d) Graphene oxide (GO)

FTIR spectra of the graphite, graphite oxide and organosilane sulfonated graphene oxide were obtained to confirm the presence of different functional groups on the graphene nanosheets (Figure 4). The graphite has two peaks at 3430 cm^{-1} (O–H stretching vibrations due to the adsorbed water) and 1610 cm^{-1} (aromatic C=C, skeletal vibrations of graphitic domains). Large amounts of oxygen-containing functional groups are found in the FTIR spectrum of graphite oxide nanosheets. The strong absorption bands at 3428, 2923, 1729, 1628, 1385, and 1121 cm^{-1} for graphite oxide confirm the existence of –OH, C–H, C=O in COOH, unoxidized graphitic skeletal domains (C=C aromatic) and the adsorbed water molecules, [71] carboxylic C–OH stretching and C–O stretching vibrations functional groups, respectively. [72] These results are in good agreement with the structure and morphology of Graphite oxide and confirm the successful oxidation of graphite. Functionalization with aryl SO$_3$H does not change the structure of the Graphite oxide, as shown in Fig. 4c. The FTIR analysis in Fig. 4c indicates that aryl sulfonic acid groups were successfully introduced into GO sheets. The strong absorption peaks at 1159 and 1230 cm^{-1} assigned to the symmetric and asymmetric stretching vibrations of S=O in –SO$_3$H group, respectively. [73] SSi–GO also exhibits additional bands at 1023 and 692 cm^{-1} which is indicated by S–phenyl and S–O groups, confirming the presence of aryl SO$_3$H groups covalently bonded to the graphene sheet. A broad peak at 3228 cm^{-1} corresponded to –OH groups on the surface and also –SO$_3$H. Additionally, the band stretching from 2888 to 2924 cm^{-1} attributed to the presence of aromatic CH groups and aliphatic C–H groups of the (CH$_2$)$_3$ chains in the CCPTES sulfanilic acid precursor. [74] The broad bands were also seen in the regions 3426 and 832 cm^{-1} which are related to aromatic NH and OOP NH groups. The strong absorption peak at 1117 cm^{-1} attributed to the Si–O stretching vibrations.
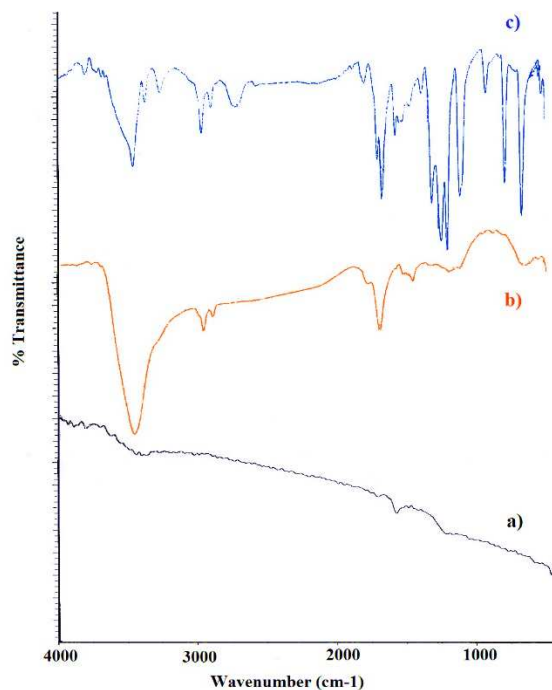

Figure 4. FT-IR spectra for (a) graphite, (b) Graphite oxide, and (c) SSi–GO

Energy dispersive spectroscopy (EDS) reveals the presence of −OSO$_3$H functional groups on the SSi-GO. EDX elemental analysis shows that the element mass ratios of carbon, nitrogen, oxygen, silicon and sulfur in the organosilane sulfonated graphene oxide are 58.32%, 17.42%, 20.79%, 0.39% and 3.09w%, respectively. The elemental analysis of SSi-GO presented that the calculated density of sulfonic acid group on the sulfonated graphene oxide is 0.96 mmol g^{-1} of –SO$_3$H based on the sulfur percentage (3.09 wt%). The O/S atom ratio (6.7 : 1) is higher than 3 : 1 owing to the presence of residual epoxide, carboxyl and hydroxyl groups on the sulfonated graphene oxide sheets.
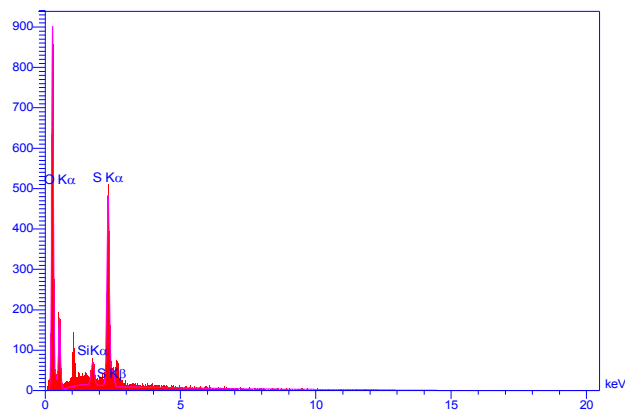

Figure 5. The EDS spectrum of SSi–GO

Furthermore, the carbon, nitrogen, oxygen, silicon and sulfur distribution maps (Figure 6) show that the SSi-GO sheets were densely and homogeneously functionalized with sulfur, reflecting the uniformity of the modification treatment.
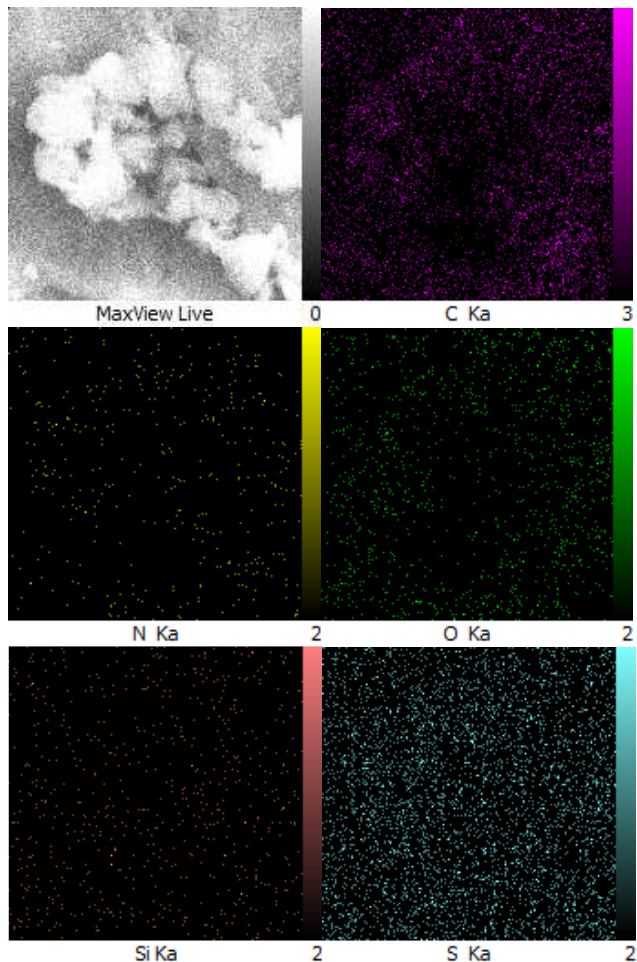

Fig 6. Elemental distribution maps in the SSi-GO region shown by EDX

Conclusions

In summary, organosilane functionalized graphene oxides (SSi–GO) were successfully synthesized and well characterized. The functionalized chemically modified organosilane graphene oxide was simply prepared via covalent functionalization with a reactive surfactant, sulfanilic acid. Hence, this study highlights that SSi–GO can be a stable, active and efficient carbocatalyst to improve the yield of pyrimidinones through one-pot multi-component reaction of aromatic aldehydes, ethyl acetoacetate (aromatic ketones) and urea or thiourea under reflux conditions. The strongly acidic aryl SO$_3$H groups are responsible for the catalytic activity and high stability of this solid acid catalyst. Moreover, the usage of SSi–GO as a BrØnsted acid and reusable carbocatalyst can be extended to other organic reactions.

Acknowledgment

Notes and references

Laboratory of Organic Compound Research, Department of Organic Chemistry, College of Chemistry, University of Kashan, P.O. Box: 87317-

51167, Kashan, Islamic Republic of Iran, Tel.: +98-(0)31-5591-2320; Fax: +98-(0)31-5591-2397, e-mail: Safari@kashanu.ac.ir

References

1   W. S. Hummers, R. E. Offeman, *J. Am. Chem. Soc.* 1958, **80**, 1339.

2   N. I. Kovtyukhova, P. I. Olliver, B. R. Martin, T. E. Mallouk, S. A. Chizhik, E. V. Buzaneva, A. D. Gorchinskiy, *Chem. Mater* 1999, **11**, 771.

3   A. B. Bourlinos, D. Gournis, D. Petridis, T. Szabó, A. Szeri, I. Dékány, *Langmuir* 2003, **19**, 6050.

4   S. Stankovich, D. A. Dikin, R. D. Piner, K. M. Kohlhass, A. Kleinhammes, Y. Y. Jia, Y. Wu, S. B. T. Nguyen, R. S. Ruoff, *Carbon* 2007, **45**, 1558.

5   H. He, J. Klinowski, M. Forster, A. Lerf, *Chem. Phys. Lett.* 1998, **287**, 53.

6   D. Li, M. B. Muller, S. Gilje, R. B. Kaner, G. G. Wallace, *Nature Nanotechnol.* 2008, **3** (2), 101.

7   A. Lerf, H. Y. He, M. Forster, J. Klinowski, *J. Phys. Chem. B.* 1998, **102**, 4477.

8   J. Kim, L. J. Cote, F. Kim, W. Yuan, K. R. Shull, J. X. Huang *J. Am. Chem. Soc.* 2010, **132**, 8180.

9   L. J. Cote, J. Kim, V. C. Tung, J. Y. Luo, F. Kim, J. X. Huang, *Pure Appl. Chem.* 2011, **83**(1), 95.

10   F. Kim, L. J. Cote, J. X. Huang, *Adv. Mater.* 2010, **22**(17), 1954.

11   T. Szabo, O. Berkesi, P. Forgo, K. Josepovits, Y. Sanakis, D. Petridis, I. Dekany, *Chem. Mater.* 2006, **18**, 2740.

12   K. A. Mkhoyan, A. W. Contryman, J. Silcox, D. A. Stewart, G. Eda, C. Mattevi, S. Miller, M. Chhowalla, *Nano Lett.* 2009, **9** (3), 1058.

13   C. Mattevi, G. Eda, S. Agnoli, S. Miller, K. A. Mkhoyan, O. Celik, D. Mastrogiovanni, G. Granozzi, E. Garfunkel, M. Chhowalla, *Adv. Funct. Mater.* 2009, **19**, 2577.

14   (a) S. Park, R. S. Ruoff, *Nat. Nanotechnol.,* 2009, **4**, 217; (b) H. Bai, Y. X. Xu, L. Zhao, C. Li, G. Q. Shi, *Chem. Commun.,* 2009, 1667.

15   (a) S. Stankovich, D. A. Dikin, G. H. B. Dommett, K. M. Kohlhaas, E. J. Zimney, E. A. Stach, R. D. Piner, S. T. Nguyen, R. S. Ruoff, *Nature*, 2006, 442, 282; (b) Q. Su, S. Pang, V. Alijani, C. Li, X. Feng and K. Müllen, *Adv. Mater.,* 2009, **21**, 3191.

16   D. R. Dreyer, H. P. Jia, C. W. Bielawski, *Angew. Chem.* 2010, **122**, 6965.

17   J. Li, G. Zhang, H. Chen, S. Wang, G. Zhang, F. Zhang, X. Fan, *Chem. Sci.* 2011, **2** (3), 484.

18   E. Lam, J. H. Chong, E. Majid, Y. liu, S. Hrapovic, A. C. W. Leung, J. H. T. Luong, *Carbon* 2012, **50**, 1033.

19   F. Liu, J. Sun, L. Zhu, X. Meng, C. Qi, F.-S. Xiao, *J. Mater. Chem.* 2012, **22**, 5495.

20   C. Su, K. P. Loh, *Acc. Chem. Res.* 2012, **46** (10), 2275.

21   a) C. H. Lu, H. H. Yang, C. L. Zhu, X. Chen, G. N. Chen, *Angew. Chem.* 2009, **121** (26), 4879; b) S. J. He, B. Song, D. Li, C. F. Zhu, W. P. Qi, Y. Q. Wen, L. H. Wang, S. P. Song, H. P. Fang, C. H Fan, *Adv. Funct. Mater.* 2010, **20**, 453.

22   Z. Liu, J. Robinson, X. M. Sun, H. J. Dai, *J. Am. Chem. Soc.* 2008, **130**, 10876.

23   L. Zhang, J. Xia, Q. Zhao, L. Liu, Z. Zhang, *Small* 2010, **6**, 537.

24   X. Sun, Z. Liu, K. Welsher, J. T. Robinson, A. Goodwin, S. Zaric, H. Dai, *Nano Res.* 2008, **1**, 203.

25   L. Cui, Y. Song, G. Ke, Z. Guan, H. Zhang, Y. Lin, Y. Huang, Z. Zhu, C. J. Yang, *Chem. Eur. J.* 2013, **19** (32), 10442.

26   H. Kim, R. Namgung, K. Singha, I. K. Oh, W. J. Kim, *Bioconjugate chem.* 2011, **22**(12), 2558.

27   J. T. Robinson, S. M. Tabakman, Y. Liang, H. Wang, H. S. Casalongue, D. Vinh, H. Dai, *J. Am. Chem. Soc.* 2011, **133**, 6825.

28   L. Wang, K. Lee, Y. Y. Sun, M. Lucking, Z. Chen, J. J. Zhao, S. B. Zhang, *ACS Nano* 2009, **3**, 2995.

29   J. Zhao, S. Pei, W. Ren, L. Gao, H. M. Cheng, *Acs Nano*, 2010, **4** (9), 5245.

30   C. Chen, W. Cai, M. Long, B. Zhou, Y. Wu, D. Wu, Y. Feng, *ACS Nano* 2010, **4**, 6425.

31   H. Zhang, X. Lv, Y. Li, Y. Wang, J. Li, *ACS Nano* 2010, **4**, 380.

32   J. Liu, H. Bai, Y. Wang, Z. Liu, X. Zhang, D. D. Sun, *Adv. Funct. Mater.* 2010, **20**, 4175.

33   G. Eda, M. Chhowalla, *Adv. Mater,* 2010, **22** (22), 2392.

34   J. Balapanuru, J. X. Yang, S. Xiao, Q. Bao, M. Jahan, L. Polavarapu, J. Wei, Q. H. Xu, K. P. Loh, *Angew. Chem., Int. Ed.* 2010, **49**, 6549.

35   D. A. Dikin, S. Stankovich, E. J. Zimney, R. D. Piner, G. H. B. Dommett, G. Evmenenko, S. T. Nguyen, R. S. Ruoff, *Nature* 2007, **448**, 457.

36   L. Fan, C. Luo, M. Sun, X. Li, H. Qiu, *Colloids Surf. B*, 2013, **103**, 523.

37   S. M. Kang, S. Park, D. Kim, S. Y. Park, R. S. Ruoff, H. Lee, *Adv. Funct. Mater,* 2011, **21** (1), 108.

38   a) Z. Luo, P. M. Vora, E. J. Mele, A. C. Johnson, J. M. Kikkawa, *Appl. Phys. lett*, 2009, **94** (11), 111909. b) Q. Mei, K. Zhang, G. Guan, B. Liu, S. Wang, Z. Zhang, *Chem. Commun.*, 2010, **46** (39), 7319.

39   M. C. Etienne, S. Cheradame, J. L. Fischel, P. Formento, O. Dassonville, N. Renee, M. Schneider, A. Thyss, F. Demard, G. Milano, *J. Clin. Oncol.* 1995, **13**, 1663.

40   V. I. Saloutin, Y. V. Burgat, O. G. Kuzueva, C. O. Kappe, O. N. Chupakhin, *J. Fluorine Chem.* 2000, **103**, 17.

41   A. I. McDonald, L. E. Overman, *J. Org. Chem.* 1999, **64**, 1520.

42   C. O. Kappe, *Eur. J. Med. Chem.* 2000, **35**, 1043.

43   H. L. Luo, W. Yang, Y. Li, S. F. Yin, *Chem. Nat. Compd.* 2010, **46** (3), 412.

44   G. C. Rovnyak, S. D. Kimball, B. Beyer, G. Cucinotta, J. D. Dimarco, J. ougoutas, A. Hedberg, M. Malley, J. P. McCarthy, R. Zhang, S. Moreland, *J. Med. Chem.* 1995, **38** (1), 119.

45   P. Biginelli, *Gazz. Chim. Ital.* 1893, **23**, 360.

46   K. R. Koch, P. F. Krause, *J. Chem. Ed.,* 1982, **59** (11), 973.

47   D. R. Dreyer, S. Park, C. W. Bielawski, R. S. Ruoff, *Chem. Soc. Rev.* 2010, **39**, 228.

48   R. Bissessur, S. F. Scully, *Solid State Ionics* 2007, **178**, 877.

49   M Saikia, D Bhuyan, L Saikia, *Applied Catal. A: General* 2015, DOI: 10.1016/j.apcata.2015.05.021.

50   D. Elhamifar, F. Hosseinpoor, B. Karimi, S. Hajati, *Microporous Mesoporous Mater.* 2015, **204**, 269.

51   M. S. SushilkumarDhanmane, *Chem. Mater. Res.* 2015, **7** (3), 27.

52   Y. Zhao, Y. Zhao, J. Zhang, H. Liu, L. Liang, *Indian J. Chem.* 2015, **45B**, 139.

53   E. Kolvari, N. Koukabi, O. Armandpour, *Tetrahedron* 2014, **70**, 1383.

54   F. Hatamjafari, *J. Appl. Chem. Res.* 2015, **9** (1), 95.

55   D. Elhamifar, M. Nasr-Esfahani, B. Karimi, R. Moshkelgosha, A. Shabani, *ChemCatChem* 2014, **6**, 2593.

56   M. Pramanik, A. Bhaumik, *ACS Appl. Mater. Interfaces* 2014, **6**, 933.

57   M. liverio, P. Costanzo, M. Nardi, I. Rivalta, A. Procopio, *ACS Sustain. Chem. Eng.* 2014, **2**, 1228.

58   A. Shaabani, A. Bazgir, *Tetrahedron Lett*. 2004, **45**, 2575.

59   R. V. Yarapathi, S. Kurva, S. Tammishetti, *Catal. Commun.*, 2004, **5** (9), 511.

60   R. Tayebee, B. Maleki, M. Ghadamgahi, *Chin. J. Catal.* 2012, **33** (4), 659.

61   A. Paraskar, G. Dewkar, A. Sudalai, *Tetrahedron Lett.* 2003, **44** (16), 3305.

62   A. R. Gholap, K. Venkatesan, T. Daniel, R. Lahoti, K. Srinivasan, *Green Chem.* 2004, **6** (3), 147.

63   M. Nasr-Esfahani, S. J. Hoseini, F. Mohammadi, *Chin. J. Catal.* 2011, **32**, 1484.

64   N. Y. Fu, Y. F. Yuan, Z. Cao, S. W. Wang, J. T. Wang, C. Peppe, *Tetrahedron*, 2002, **58**, 4801.

65   C. V. Reddy, M. Mahesh, P. Raju, T. R. Babu, V. Reddy, *Tetrahedron lett.* .2002, **43**, 2657.

66   A. Rajack, K. Yuvaraju, C. Praveen, Y. Murthy, *J. Mol. Catal. A: Chem.* 2013, **370**, 197.

67   B. Liang, X. Wang, J. Wang, Z. Du, *Tetrahedron*, 2007, **63**, 1981.

68   Y. M. Ren, C. Cai, *Monatsh. Chem.,* 2009, **140** (1), 49.

69   J. J. Niu, J. N. Wang, *Electrochim. Acta* 2008, **53**, 8058.

70   W. Scholz, H. P. Boehm, *Z. Anorg. Allg. Chem.* 1969, **369** (3-6), 327.

71   T. Szabo, O. Berkesi, I. Dekany, *Carbon* 2005, **43** (15), 3186.

72   G. I. Titelman, V. Gelman, S. Bron, R. L. Khalfin, Y. Cohen, H. B. Peled, *Carbon* 2005, **43** (3), 641.

73   L. Zhang, J. Xia, Q. Zhao, L. Liu, Z. Zhang, *Small* 2010, **6**, 537.

74   Y. Si, E. Samulski, *Nano Lett.* 2008, **8**, 1679.

Graphical abstract

The acidic functionalized SSi–GO was used as highly active, selective and reusable catalyst to improve formation of pyrimidinones.